

Published in final edited form as:

*Mater Res Soc Symp Proc.* 2009 ; 1132E(1132-Z03-07): ukpmcpa27262. doi:10.1557/PROC-1132-Z03-07.

## Mapping the Micromechanical Properties of Cryo-sectioned Aortic Tissue with Scanning Acoustic Microscopy

Riaz Akhtar<sup>1</sup>, Michael J. Sherratt<sup>2</sup>, Rachel E.B. Watson<sup>3</sup>, Tribikram Kundu<sup>4</sup>, and Brian Derby<sup>1</sup>

<sup>1</sup>Manchester Materials Science Centre, School of Materials, The University of Manchester, Grosvenor Street, Manchester, M1 7HS, United Kingdom

<sup>2</sup>Tissue Injury and Repair Group, Faculty of Medical and Human Sciences, The University of Manchester, 1.581 Stopford Building, Oxford Road, Manchester, M13 9PT, United Kingdom

<sup>3</sup>Dermatological Sciences Research Group, Faculty of Medical and Human Sciences, The University of Manchester, 1.443 Stopford Building, Oxford Road, Manchester, M13 9PT, United Kingdom

<sup>4</sup>Department of Civil Engineering and Engineering Mechanics, University of Arizona, Tucson, Arizona 85721, USA

### Abstract

Although the gross mechanical properties of ageing tissues have been extensively documented, biological tissues are highly heterogeneous and little is known concerning the variation of micro-mechanical properties within tissues. Here, we use Scanning Acoustic Microscopy (SAM) to map the acoustic wave speed (a measure of stiffness) as a function of distance from the outer adventitial layer of cryo-sectioned ferret aorta. With a 400 MHz lens, the images of the aorta samples matched those obtained following chemical fixation and staining of sections which were viewed with fluorescence microscopy. Quantitative analysis was conducted with a frequency scanning or  $V(f)$  technique by imaging the tissue from 960 MHz to 1.1 GHz. Undulating acoustic wave speed (stiffness) distributions corresponded with elastic fibre locations in the tissue; there was a decrease in wave speed of around  $40 \text{ ms}^{-1}$  from the adventitia (outer layer) to the intima (innermost).

### INTRODUCTION

Elastic fibres are an abundant component of extracellular matrices in dynamic tissues such as arteries, lungs and skin [1]. They play an important mechanical role by endowing tissues, such as the aorta with resilience, permitting long-range deformability and passive recoil. These composite elastic fibres rely on an inner, highly compliant, elastin core to drive recoil, and an outer mantle of less abundant but stiffer fibrillin microfibrils [2] to anchor the fibres within the tissue. The ability of elastic fibre-rich arteries to extend and recoil more than  $3 \times 10^9$  times during the course of an average human lifetime plays a pivotal role in buffering extremes of blood pressure and hence in preserving cardiovascular function. With age and pathology, elastic fibre-rich tissues become stiffer [3], lose the ability to recoil [4] and ultimately fail [5].

We have recently used a nanoindentation analysis methodology to spatially map the mechanical properties of  $5 \mu\text{m}$  thick ferret aorta and vena cava, and related the micromechanical properties to the histological distribution of elastic fibres [6]. In this study, we use SAM to quantify variations in ferret aorta mechanical properties at a length scale of around  $10^{-6}$  m. SAM is a unique, high spatial resolution tool for the study of mechanical

properties of biological tissue, potentially allowing a direct correlation between histology and micromechanical properties of tissue. SAM uses ultra-high frequency sound vibrations (100 MHz - 1 GHz) to image materials, with the contrast related to the variation in acoustic wave speed within the tissue, which is related to the stiffness and density of the sample. The spatial resolution of the SAM is related to the wavelength of the acoustic radiation; at 1 GHz the resolution is close to  $10^{-6}$  m. This spatial resolution is considerably better than what is currently achievable through nanoindentation. Furthermore, SAM is completely non-destructive and samples are kept fully hydrated due to the coupling fluid (normally water) that has to be used between the acoustic lens and the sample.

SAM has been used in the past to characterise the mechanical properties of biological tissue [7]. However, the vast majority of this prior work has been on stiff, calcified tissues [8-11]. Furthermore, most researchers have tended to work in the frequency range of 100-500 MHz [12-14], limiting the spatial resolution achievable. All the prior studies that the authors are aware of on soft biological tissue have been conducted on chemically fixed tissue sections e.g. [15].

## EXPERIMENT

Histological cross-sections of ferret descending aorta were prepared from unfixed, OCT embedded tissue samples, which were frozen in liquid N<sub>2</sub>-cooled isopentane prior to storage at -80°C pending cryo-sectioning. Frozen, OCT-embedded specimens were secured to cryostat chucks with OCT and sectioned to nominal thicknesses of 5 μm. The samples were mounted on glass slides with known mechanical properties (Surgipath Europe Ltd, Peterborough, UK)

SAM imaging was conducted using a SAM 2000 (KSI GmbH, Heborn, Germany). Images were taken with both a 400 MHz and 1 GHz lens, with the latter used for quantitative analysis. The experiments were conducted at room temperature with distilled water used as a coupling fluid. For quantitative analysis, six images were recorded at the following frequencies: 960, 970, 980, 990, 1000 and 1010 MHz. These images were subsequently analysed off-line using the  $V(f)$  method which is outlined in the following sub-section.

Following SAM imaging, the tissue sections were fixed in 4 % paraformaldehyde solution for 10 minutes and subsequently stained with hematoxylin and eosin (H&E) following a standard procedure, and mounted in DePex Mounting Medium (Electron Microscopy Sciences, Fort Washington, PA, USA). The sections were subsequently visualised by fluorescence microscopy (Nikon Eclipse 50i) equipped with Lucia software (Version 4.82, Laboratory Imaging Ltd.).

### $V(f)$ -technique

The  $V(z)$ -method (recording of output voltage vs. defocus distance,  $z$ ), which determines the velocity of surface acoustic waves (Rayleigh waves), is commonly used to obtain quantitative measurements for engineering materials [16]. However, this technique is not suitable for soft biological specimens because it requires a very smooth specimen surface and due to the rapid attenuation of Rayleigh waves in tissue. The  $V(f)$  methodology (recording of voltage output vs. signal frequency) was developed by Kundu et al. [17,18] and is more suited to soft biological tissues because it allows quantitative measurements to be made from full images of the tissue. Crucially, for rough biological specimens the method accounts for variations in surface topography. This technique exploits the interference that is generated within thin tissue specimens mounted on glass slides. By imaging near the focal plane with no defocus ( $z = 0$ ), only normally incident P-waves have to be considered. These waves are reflected by both the tissue-substrate and tissue-coupling

fluid interfaces. The returned signal amplitude is an interference of these reflected signals that is determined by the tissue and substrate properties as well as the tissue thickness. As the substrate properties are known, the unknown parameters that control the reflected wave amplitude are thickness, density, wave speed and attenuation of the tissue. To obtain these four unknown parameters at any pixel position one needs to have at least four equations to solve for the four unknowns. These four equations can be obtained by measuring reflected wave amplitude at four different frequencies. However, to increase accuracy, six frequencies (and therefore equations) are used to solve the four unknowns. Thus, the signal voltage amplitude ( $V$ ) is recorded for six different frequency ( $f$ ) values at every pixel point and these are used to determine the acoustic wave speed. The acoustic wave speed cannot be solved analytically and an optimization method based on the Simplex algorithm is used to determine the best solution in terms of specimen thickness, attenuation and density. [17]

The SAM images were analysed using STAN (Soft Tissue Analysis) software developed at Aarhus University Hospital (Denmark), which is based on underlying DOS software developed by Kundu [19]. Ten line measurements were made which spanned the entire cross-section of an aorta section, from the adventitial to the intimal layer.

### Statistical Analysis

For each line, the raw datasets were smoothed using an adjacent averaging algorithm to eliminate noise and was binned at 10 pixel intervals. Binned regression lines (wave speed versus distance) were analysed using Analysis of Variance (ANOVA) with a data analysis software package (statistiXL, Broadway Nedlands, Western Australia) to determine whether the ten separate lines shared a common slope and intercept.

## DISCUSSION

With a 400 MHz lens the spatial resolution achievable with SAM is approximately  $4\ \mu\text{m}$  and the tissue organisation visualised by wave speed contrast resembled the histological appearance of H&E stained sections viewed with fluorescence microscopy; in both images elastic fibres were clearly visible (Figure 1).

As with differential staining methods such as Weigert's elastin stain, H&E staining followed by fluorescence microscopy can differentially visualise elastic fibre components in tissue [20]. Thus, the foremost advantage of using SAM to study biological tissue is that mechanical data, obtained in the absence of chemical interventions such as dehydration, fixation and paraffin embedding, may be directly mapped to the histological tissue organisation.

Quantitative analysis was only possible with the 1 GHz lens, which is a broadband lens and hence frequency could be varied in small increments as required for the  $V(f)$  method. However, at 1 GHz, the spatial resolution of the SAM is much higher and hence the images are more complex, incorporating both cellular and extracellular detail (Figure 2a). Despite the substantial contrast in these 1 GHz images, acoustic wave speed correlate well with fluorescence images showing significant contrast variation from the elastic fibres (Figure 2).

Figure 2 suggests that the variation in wave speed correlates with the elastic fibre distribution; thus, the highest wave speeds (stiffest regions) are associated with the position of elastic fibres. Smooth muscle cells are situated between the elastic fibres and are thought to result in the lowest wave speeds.

ANOVA was used to statistically compare the regression lines of the binned data. ANOVA showed that the slopes of the 10 lines did not differ significantly and therefore a common

slope was determined (-0.03). Similarly, the intercepts were not significantly different and a common intercept was 1.83.  $P$  was 0.71 ( $F = 0.7$ ) and 0.52 ( $F = 0.92$ ) for the slope and intercept respectively. All of the lines were then averaged to provide a mean relationship between wave speed and distance from the adventitial layer (Figure 3).

The progressive decrease in wave speed as a function of distance from the adventitial layer of the aorta (Figure 3) correlates well with the distribution of extracellular matrix and cellular components and also matches the trend found using nanoindentation. [6]. The outer (adventitial) layer is known to be relatively acellular and rich in collagen, the stiffest component of large blood vessels. The prominent medial layer is rich in elastic fibres which provide the tissue with compliance, and in ferret aorta an increase in elastic fibre density was observed with distance from the adventitial layer. Finally, the intimal layer is composed entirely of highly compliant endothelial cells. Due to the non-parallel arrangement of the elastic fibres, there is some scatter in the averaged data. A larger sample size with a greater number of line measurements may improve this relationship.

Jensen et al. [21] have reported that the  $V(f)$  methodology can be used to discriminate between the elastic properties of differing histological layers of heart valve tissue. However, each histological layer for which they provided average data spanned several hundred microns. Furthermore, the tissue used in their study was embedded in paraffin and fixed in formaldehyde. We have shown that it is possible to examine pixel-by-pixel (equating to a spatial resolution of  $\sim 1$  micron) level variations in acoustic wave speed and to relate these variations to microstructural components such as elastic fibres. Furthermore, the variations in wave speed as observed in  $10 \mu\text{m}$  increments fits well with the known tissue structure. The binned data (Figure 3) shows approximately a  $40 \text{ ms}^{-1}$  decrease in wave speed from the stiffest outer (adventitial) to the innermost (intimal) layer. Jensen *et al.* [21] found that there was approximately a  $60 \text{ ms}^{-1}$  decrease in wave speed from the stiffest histological layer to the least stiff. Although the exact compositions and organisation of aorta and heart valve tissue differ, the molecular constituents are similar with collagen being the stiffest component and elastin providing the tissue with compliance.

At the ultra-high frequencies used in this study, viscosity is not thought to have an effect on the acoustic wave speed values of the tissue and therefore the wave speed values reflect tissue elasticity. Acoustic attenuation, which was not presented in this paper, is determined by absorption of sound within the tissue, and is therefore more closely related to tissue viscosity [22].

## CONCLUSIONS

SAM can be used to determine micron-scale variations in the mechanical properties of soft biological tissue using the frequency scanning or  $V(f)$  technique. The progressive drop in wave speed determined as a function of distance from the outer adventitial layer of the aorta matches well with nanoindentation data.

## Acknowledgments

The authors are grateful to Carsten Riis and Aarhus University Hospital, Denmark for granting use of STAN software. EPSRC, Research into Ageing and BHF must be acknowledged for funding. Drs Helen Graham and Andrew Trafford must be thanked for providing the tissue samples.

## REFERENCES

1. Kielty CM, Sherratt MJ, Shuttleworth CA. *J. Cell Sci.* 2002; 115:2817. [PubMed: 12082143]

2. Sherratt MJ, Baldock C, Haston JL, Holmes DF, Jones CJP, Shuttleworth CA, Wess TJ, Kielty CM. *J. Mol. Bio.* 2003; 332:183. [PubMed: 12946356]
3. Lai-Fook SJ, Hyatt RE. *J. Appl. Physiol.* 2000; 89:163. [PubMed: 10904048]
4. Escoffier C, de Rigal J, Rochefort A, Vasselet R, Leveque JL, Agache PG. *The Journal of investigative dermatology.* 1989; 93:353. [PubMed: 2768836]
5. Lederle FA. *Ann. of Intern. Med.* 2003; 139:516. [PubMed: 13679330]
6. Akhtar R, Sherratt MJ, Bierwisch N, Derby B, Mummery PM, Watson REB, Schwarzer N. *MRS Symp. Proc.* 2008; 1097E:GG01.
7. Daft CM, Briggs GA. The elastic microstructure of various tissues. *J. Acoust. Soc. Am.* 1989; 85:416. [PubMed: 2921421]
8. Hasegawa K, Turner CH, Recker RR, Wu E, Burr DB. *Bone.* 1995; 16:85. [PubMed: 7742089]
9. Litniewski J. *Ultrasound Med. Biol.* 2005; 31:1361. [PubMed: 16223639]
10. Raum K, Kempf K, Hein HJ, Schubert J, Maurer P. *Dent. Mater.* 2007; 23:1221. [PubMed: 17178152]
11. Saied A A, Raum K, Leguerney I, Laugier P. *Bone.* 2008; 43:187. [PubMed: 18407822]
12. Hozumi N, Kimura A, Terauchi S, Nagao M, Yoshida S, Kobayashi K, Saijo Y. *Proc. IEEE Ultrasonics Symp.* 2005; 1:170.
13. Hattori K, Sano H, Saijo Y, Kita A, Hatori M, Kokubun S, Eiji E. *J. Pediatr. Orthop. B.* 2007; 16:357. [PubMed: 17762676]
14. Saijo Y, Hozumi N, Lee C, Nagao M, Kobayashi K, Oakada N, Tanaka N, dos Santos Filho E, Sasaki H, Tanaka M, Yambe T. *Ultrasonics.* 2006; 44:e51. [PubMed: 16844175]
15. Saijo Y, Nitta S-i, Jørgensen CS, Falk E. *Proc. SPIE.* 2001; 4335:228.
16. Briggs, GAD. *An Introduction to Scanning Acoustic Microscopy.* Oxford University Press; 1985.
17. Kundu T, Bereiter-Hahn J, Karl I. *Biophys. J.* 2000; 78:2270. [PubMed: 10777725]
18. Jørgensen CS, Hasenkam JM, Kundu T. *Proc. SPIE.* 2001; 4335:244.
19. Kundu T. *J. Appl. Mech-T ASME.* 1992; 59:54.
20. de Carvalho HF, Taboga SR. *Histochem. Cell. Biol.* 1996; 106:587. [PubMed: 8985747]
21. Jensen AS, Baandrup U, Hasenkam JM, Kundu T, Jørgensen CS. *Ultrasound Med. Biol.* 2006; 32:1943. [PubMed: 17169706]
22. Liang H-D, Blomley MJK. *Br. J. Radiol.* 2003; 76:S140. [PubMed: 15572336]

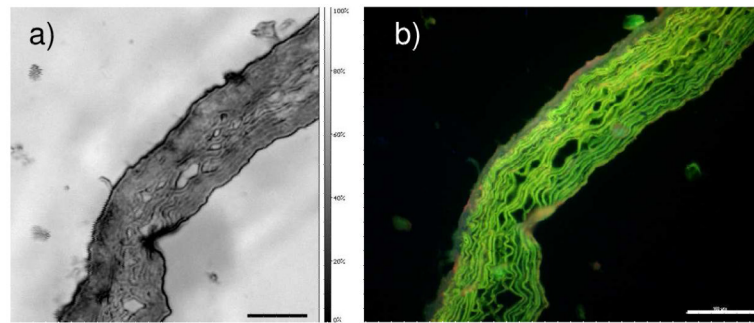


**Figure 1.** Ferret aorta section imaged first by with (a) 400 MHz SAM and (b) subsequently by fluorescence microscopy following paraformaldehyde-fixation and H&E staining. Scale bar represents 100  $\mu\text{m}$ .

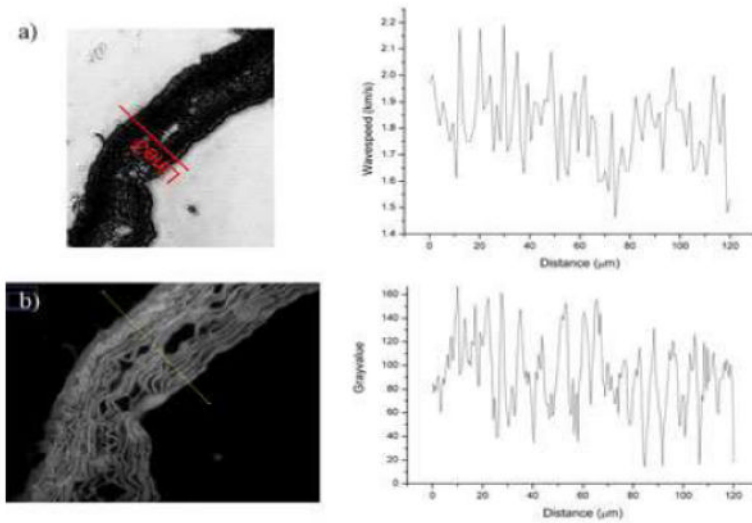


**Figure 2.**

**a)** 1 GHz fluorescence image with plot of undulating acoustic wavespeed (stiffness) distribution which corresponds with the elastic fibre locations as demonstrated by **b)** Grayscale fluorescence image with plot showing similar undulation of grey values. The distance '0 μm' in both plots represents the outermost (adventitial) edge of the tissue (leftmost in the figures).

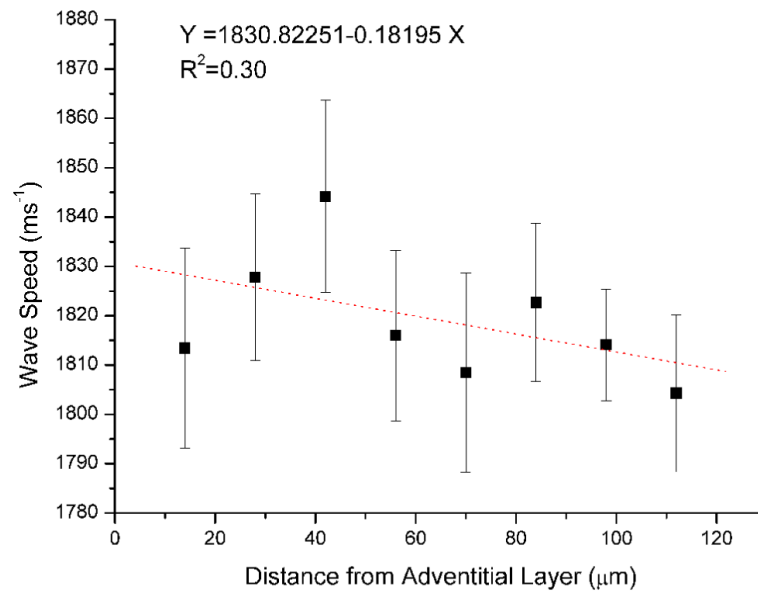


**Figure 3.** Plot showing mean wave speed versus distance from the outer adventitial layer. Error bars represent standard error of the mean.